

ATOMIC AND MOLECULAR PHYSICS

Dedicated to Prof. Ioan-Iovitz Popescu's 75th Anniversary

TOWARDS AN OPTICAL LATTICE CLOCK BASED
ON NEUTRAL MERCURY

CIPRIANA MANDACHE¹, MICHAEL PETERSEN², DANIEL V. MAGALHÃES³,
OUALI ACEF², ANDRE CLAIRON², SEBASTIEN BIZE²

¹ National Institute for Laser Physics, Plasmas and Radiation, Plasmas and Nuclear Fusion
Laboratory, Bucharest, Magurele, PO Box MG 7, Romania

² LNE-SYRTE, Observatoire de Paris, UMR CNRS 8630, 61 avenue de l'Observatoire,
75014 Paris, France

³ Instituto de Física de São Carlos, USP - PO Box 369, 13560-970, São Carlos, SP, Brazil
Email: cipriana@infim.ro

(Received February 6, 2008)

Abstract. We are investigating the possibilities of using neutral mercury as a new species to realize a highly accurate atomic clock using the non-perturbing dipole lattice trapping scheme. Typically, accuracy below 10^{-17} is targeted, which would make neutral mercury an interesting candidate for a redefinition of the SI second. This paper presents our on-going work towards the realization of an optical lattice clock using neutral mercury. We will describe a 254 nm laser source delivering several hundreds of milliWatts at this wavelength with a suitably low frequency noise for laser cooling and magneto-optic trapping. We will describe our vacuum system for magneto-optic trap and report on the status of our work regarding magneto-optic trapping of mercury. We will also describe our clock laser at 266 nm.

Key words: optical frequency standards, cooling atoms, ultra-stable cavity.

1. INTRODUCTION

In the past few years, intense efforts have been devoted worldwide to the development of a new generation of atomic clocks based on optical transitions. These efforts have been re-enforced by the advent of the optical frequency comb technology. For instance, optical clocks based on trapped $^{199}\text{Hg}^+$ and Al^+ ions are now clearly surpassing atomic fountain clocks with accuracies below 10^{-16} [1]. Optical clocks using neutral atoms are reaching accuracies near or below 10^{-15} [2], [3]. These achievements have started impacting the applications of high accuracy atomic clocks. For example, recent absolute frequency measurements of the $^{199}\text{Hg}^+$ optical clock are leading to improved test of the stability of the fine

structure constant α [4]. Several atomic transitions in the optical domain are now recognized by BIPM as secondary representations of the SI second. In this paper we are introducing a project aiming to develop an optical lattice clock [5, 6] based on neutral mercury. Like for other optical lattice clocks, the goal is to combine the advantages of a trapped ion, where the clock transition is probed in the Lamb-Dicke regime, with those of neutral atoms, where a large ensemble of atoms can be sampled simultaneously. As shown below, several atomic properties of Hg are making it an interesting candidate for reaching ultimate accuracy. Also, introducing a new atom with a relatively high sensitivity to α variation [7] will increase the number of possibilities to perform fundamental physics tests. In the future, LNE-SYRTE will operate two microwave clocks (based on ^{87}Rb and ^{133}Cs hyperfine transitions [8, 9]) and two optical lattice clocks based on Sr and Hg.

2. PROPERTIES OF MERCURY RELEVANT TO AN OPTICAL LATTICE CLOCK

2.1. THE ADVANTAGES AND DISADVANTAGES OF MERCURY

Mercury is a rather heavy atom having an atomic number of 80 and an average atomic mass of 200.59. Already this makes it necessary to use a non-negligible amount of laser power to laser-cool the atoms. Mercury has seven natural abundant isotopes, 2 fermions and 5 bosons (see Table 1).

Mercury has 2 fermionic and 4 bosonic abundant isotopes with an alkaline-earth like atomic structure (similar to Ca, Sr, Yb). Both fermions (^{199}Hg , ^{201}Hg) have a weakly allowed intercombination line ($^1\text{S}_0$ - $^3\text{P}_0$) with a ~ 100 mHz natural line-width at 266 nm [11] and an accessible “magic wavelength”, at which a dipole field does not disturb this “clock” transition [12, 13]. Alternatively, using a static magnetic field to quench the $^3\text{P}_0$ metastable state, it is possible to use the same transition in the bosonic isotopes [14]. The blackbody radiation induced frequency

Table 1

The natural isotopes of mercury [10]

Isotope	Abundance (%)	Nuclear spin	Magnetic moment
196	015	0	0
198	10.1	0	0
199	17.0	1/2	+0.5059
200	23.1	0	0
201	13.2	3/2	-0.5602
202	29.6	0	0
204	6.85	0	0

shift may ultimately be the main limiting factor to the accuracy of optical lattice clocks. In this respect, mercury has the advantage of having a low sensibility to this effect (~ 20 times smaller than Sr, ~ 10 times smaller than Yb and Ca [15]). This and other advantages of neutral mercury are making this atom a credible candidate for realizing an atomic clock with the highest level of performance. Typically, accuracy below 10^{-17} is targeted, which would make neutral mercury an interesting candidate for a redefinition of the SI second. Also, among neutral atoms used in atomic clocks, mercury has a high sensitivity to a putative variation of the fine-structure constant [16].

Mercury has a vapor pressure of about a factor of 10^3 higher than Cs and Rb. At room temperature mercury has a vapor pressure of 0.3 Pa and for the purpose of laser cooling this is largely sufficient and therefore no oven is needed. A vapor pressure between 10^{-5} and 10^{-4} Pa, well suited for a vapor cell magneto-optic trap, is met near $-55 \pm 5^\circ\text{C}$, a temperature which is easily reached in vacuum with Peltier thermoelectric coolers. Pumping of mercury can be done for instance with a cold surface. The vapor pressure goes down to 10^{-7} Pa near -80°C [17]. Like strontium or ytterbium, mercury has an alkaline-earthlike electronic structure shown in Fig. 1. The ground 6^1S_0 state is a singlet state with no spin for the bosonic

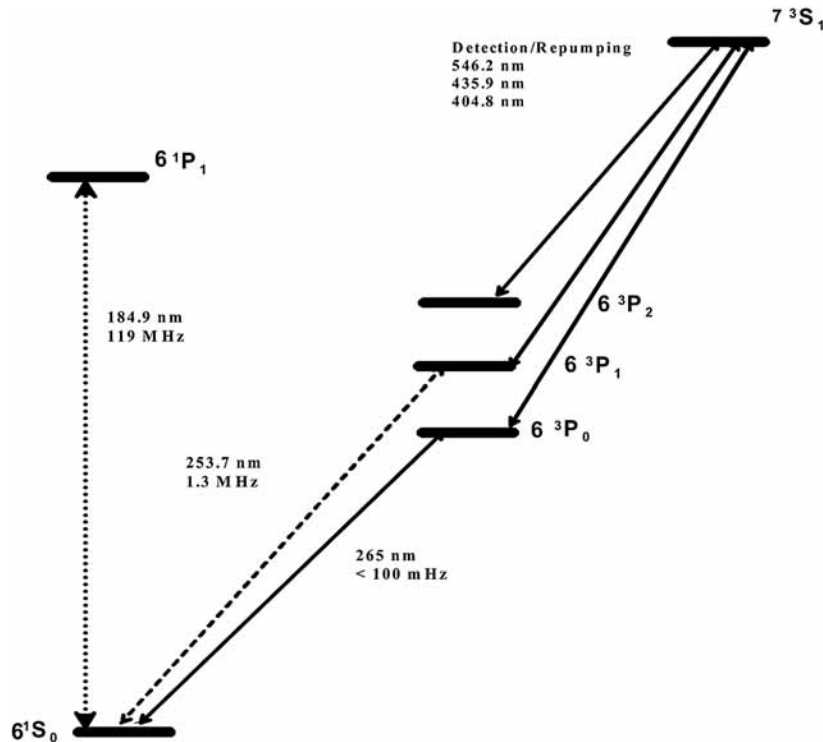


Fig. 1 – The lowest energy levels of mercury.

isotope and a purely nuclear spin of 1/2 and 3/2 for the fermionic isotopes ^{199}Hg and ^{201}Hg (Table 1). The strongly allowed transition to 6^1P_1 has a wavelength of 185 nm and is not well suited for laser cooling because this wavelength is very difficult to synthesize and because the short lifetime of the 6^1P_1 state of 1.3 ns corresponds to quite a high Doppler temperature of 2.8 mK. Instead, the inter-combination transition to the 6^3P_1 has a wavelength of 254 nm which is less challenging to synthesize. Also, the natural linewidth of 1.3 MHz corresponds to a favorable Doppler temperature of 31 μK while being strong enough for magneto-optic trapping. The saturation intensity of this transition is 10 mW cm^{-2} .

2.2. BLACKBODY RADIATION SHIFT

Blackbody radiation shift is a significant shift for all atomic frequency standards both in the microwave and the optical domains. What makes mercury an even better candidate for the dipole scheme is its relatively low sensibility to blackbody radiation as is shown in Table 2. For instance, it is one of the largest shifts in atomic fountain clocks (-1.7×10^{-14} at 300 K) and requires difficult measurements to be controlled to better than the percent level [18]. It is the largest shift in optical lattice clock based on ^{87}Sr (-5.5×10^{-15} at 300 K [19]). In the future, the blackbody radiation shift could be the limiting factor to the accuracy of several optical clocks at the level of a few parts in 10^{17} . One of the interesting features of Hg is its blackbody radiation shift smaller than for other atoms considered for optical lattice clocks. The shift is estimated to be -2.4×10^{-16} at 300 K [12], 10 times smaller than for Yb and 20 times smaller than for Sr. Blackbody radiation shift at 300 K in Hg^+ and In^+ is significantly smaller (factor of ~ 3). It is much smaller [20] in Al^+ (factor of 30).

Table 2

Atom transition fractional shift due to blackbody radiation at 300 K

Atom	Transition	Fractional shift due to blackbody radiation at 300 K
Cs	$F=3 \rightarrow F=4$	$-1.7 \cdot 10^{-14}$
Rb	$F=1 \rightarrow F=2$	$-1.3 \cdot 10^{-14}$
Sr	$^1\text{S}_0 \rightarrow ^3\text{P}_0$	$-5.5 \cdot 10^{-15}$
Ca	$^1\text{S}_0 \rightarrow ^3\text{P}_1$	$-2.2 \cdot 10^{-15}$
Yb	$^1\text{S}_0 \rightarrow ^3\text{P}_0$	$-2.4 \cdot 10^{-15}$
Mg	$^1\text{S}_0 \rightarrow ^3\text{P}_0$	$-3.9 \cdot 10^{-16}$
Hg	$^1\text{S}_0 \rightarrow ^3\text{P}_0$	$-2.4 \cdot 10^{-16}$

2.3. SENSITIVITY TO α VARIATION

One of the principal reasons to make clocks of different atomic species with good stabilities and accuracies is to be able to measure the stability of the fundamental constants such as the fine-structure constant α . It is advantageous that the mercury 265.6 nm transition has a rather high sensitivity to α : $d\ln(\omega_{at}) = 0.81d\ln(\alpha)$.

2.4. MAGIC WAVELENGTH AND DIPOLE TRAPPING

Feasibility of the optical lattice clock scheme relies on the existence of a so-called magic wavelength, where the ac-polarizabilities of both clock states are equal. For mercury, such magic wavelength exists between the two strongly allowed transitions from 6^3P_0 to 7^3S_1 at 405 nm and from 6^3P_0 to 6^3D_1 at 297 nm [12]. A first calculation, in 2006 gave a magic wavelength of 342 nm [13]. A more recent calculation gives 360 nm [21]. The recoil frequency corresponding to this wavelength is 7.7 kHz. To achieve a trap depth of 1 recoil, the required intensity is $5.1 \text{ kW}\cdot\text{cm}^{-2}$ for a traveling wave.

3. TOWARDS COOLING AND TRAPPING OF MERCURY

Magneto-optical trapping (MOT) of neutral mercury is a prerequisite for the realization of an atomic clock. It is also an attractive goal to laser cool a new atomic species which often gives access to better knowledge of atomic properties. This is particularly true for mercury with at least 6 practically usable isotopes.

3.1. MOT CHAMBER

In our proposed design, the MOT will be loaded by a 2 dimensional magneto-optical trap (2D-MOT) [22]. The high vapor pressure of mercury makes it possible to load this 2D-MOT from a background vapor while keeping the vacuum chamber at room temperature as it is done for Cs or Rb. The Hg background pressure will be held at an appropriate level for the 2D-MOT (10^{-5} and 10^{-4} Pa) using the Hg source described in the next subsection. A 1.5 mm diameter and 10 mm long hole will let atoms effusing horizontally from the 2D-MOT towards the center of the MOT, while strongly reducing the conductance for the background gas. The MOT center is 7 cm away from the output of the 2D-MOT. Having in mind the clock application, the vacuum chamber parts are made of non-magnetic material (TA6V titanium alloy). The windows are made with AR-coated UV grade fused silica

which transmits the cooling and clock wavelengths. Water cooled MOT coils are designed to create a magnetic field gradient of $\sim 75 \text{ G}\cdot\text{cm}^{-1}$ for a current of 10 A and a power dissipation of $\sim 50 \text{ W}$. Values are similar for the 2DMOT coils with a dissipated power of $\sim 150 \text{ W}$. According to some preliminary numerical calculations, the optimum gradient is about $\sim 60 \text{ G}\cdot\text{cm}^{-1}$, a quite high value due to the heavy atomic mass. In the present form, the vacuum chamber includes a time of flight zone which should help optimizing and studying cooling and trapping.

3.2. MERCURY SOURCE

Since mercury has an exceptionally high vapor pressure of 0.3 Pa at room temperature, the source of mercury for the 2D-MOT is cooled down to reduce and control the mercury pressure. Liquid mercury is placed in a small copper bowl glued to the cold surface of a two-stage Peltier thermoelectric cooler placed inside the vacuum. The hot side of the thermoelectric cooler is attached to a water-cooled block of copper whose temperature is maintained near 10°C . The Peltier element can sustain a temperature difference of 81°C which is more than enough to bring the mercury temperature to the required $-55 \pm 5^\circ\text{C}$. In addition to the mercury source, the 2D-MOT chamber includes a getter pump to pump other residual gases. So far experiments show that we can release and recapture mercury by controlling the power to the Peltier element although the recapture process is slower and not completely perfect. This is probably due to mercury being captured in the walls of the vacuum chamber. No particular care has been taken to purify mercury. However, the noticeable release of nitrogen and hydrogen by the mercury source remains at least one order of magnitude smaller than the released mercury and should not be detrimental to the 2D-MOT. Additionally, the getter pump seems to tolerate exposure to mercury vapor. Notice that pumping of mercury in the MOT chamber is achieved by a device similar to the mercury source. A copper surface is maintained below -100°C by means of a 6-stage Peltier thermoelectric cooler placed inside the vacuum. This pump is complemented by a getter pump.

3.3. COOLING LIGHT SOURCE

One of the challenging tasks in this project is to synthesize the 254 nm light for laser cooling and atomic detection on the $1 \text{ S}_0 \rightarrow 3 \text{ P}_1$ transition. Typically, several 100 mW of power are required. Additionally, in order to reach the lowest temperature, the laser linewidth and frequency fluctuations must be a small fraction of the natural linewidth of 1.3 MHz at 254 nm which is significantly more constraining than for instance Rb (6 MHz natural linewidth at 780 nm). The laser source is based on a near infrared diode-pumped Yb:YAG thin-disk laser. This

laser delivers 7 W of CW single frequency laser light at 1015 nm. This light is frequency doubled in a commercial cavity-enhanced second harmonic generation (SHG) unit using a 90° phase matched LBO crystal at $\sim 216^\circ\text{C}$. Up to 3 W have been obtained at 508 nm. The second SHG is performed with a home made system inspired by the work of [23]. An AR-coated 7 mm long β -barium borate (BBO) crystal is used, for which type I angle-tuned phase matching is achieved at $\theta = 51.2^\circ$. The ring cavity is made of one flat 98.5% reflecting input coupler, of one flat mirror and two curved mirrors with 50 mm radius of curvature. The round trip length is 241 mm and the size of the waist in the crystal is $\sim 28 \mu\text{m}$. Light at 254 nm is extracted through one of the curved mirrors which is coated for maximum transmission at this wavelength and made of UV grade fused silica. More than 600 mW of continuous light at 254 nm has been obtained from this system. The next step to make this source suitable for laser cooling is to stabilize the laser to the atomic line. In order to do so, we perform saturated absorption spectroscopy. Thanks to the high vapor pressure of mercury, a room temperature cell with an interaction length of 1 mm is well suited for the task. Cells have been realized by condensing a small quantity of purified mercury in a commercially available quartz cell. For probing the cell, a small fraction of light reflecting off the output coupler and transmitted through the input coupler (also made of UV grade fused silica) was used. A Doppler free spectrum was observed for the six abundant isotopes, as exemplified in Fig. 2 with the 200Hg spectrum line. The Doppler

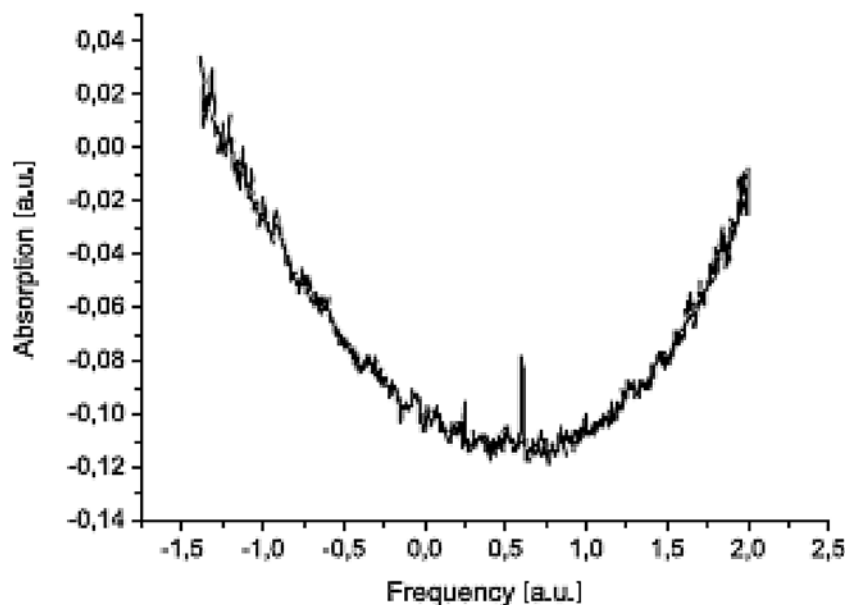


Fig. 2 – Measured saturated absorption spectrum of 200Hg at 254 nm. The measurement is performed on room temperature quartz cell with an interaction length of 1 mm.

linewidth is close to 1 GHz FWHM. Using a 5 mm cell, the Doppler spectrum of the 0.15% abundant ^{196}Hg isotope was also observed. At this point, the next step would have been to stabilize the laser light to the saturated absorption peak by acting on the PZT driven output coupler of the thin-disk laser. Unfortunately, a failure of this laser stopped us from completing this step. The laser has been under repair for several months. The previously described steps already demonstrate the feasibility of a laser source suitable for cooling mercury. This work will be pursued when the laser returns. Similar work has been done simultaneously, as reported in [24].

4. DEVELOPMENT OF AN ULTRA STABLE LASER SOURCE AT 265.6 nm

Exciting the clock $^1S_0 \rightarrow ^3P_0$ transition requires an ultra stable laser source at 265.6 nm. About 10 mW of power is required to reach a Rabi frequency of several kHz over the entire size of the MOT. This excitation rate should be sufficient for preliminary investigations of the clock transition on atoms free-falling from the MOT as done in [25, 26]. In the long run, performing high resolution spectroscopy in the dipole lattice trap and running the clock requires much less power. To synthesize this wavelength, a narrow-line Yb-doped fiber laser is used at 1062.5 nm (4 times the required wavelength). Such laser has intrinsically low frequency noise and therefore constitutes a convenient starting point for an ultra stable light source. The light from this laser will be stabilized to a reference Fabry-Perot cavity and sent to an optical frequency comb for frequency measurements and comparisons with other clocks. As a second step, the stabilized light is amplified and frequency doubled twice.

4.1. CLOCK LASER

The 1062.5 nm Yb-doped fiber laser is a commercially available laser [27]. Due to the small tunability of these lasers, the laser must be customized to meet the required wavelength. The wavelength can be temperature-controlled (slow tuning) in a ~ 650 pm range around 1062.467 nm. Fast (several 10 kHz bandwidth), small amplitude tuning is achieved with a PZT. Thanks to an output amplifier stage, the laser has an adjustable output power up to 200 mW (PM fiber coupled). As a first step, we have carefully characterized the noise properties of the free-running fiber laser. Both the relative intensity noise (RIN) and the frequency noise have been measured at several output powers. The RIN is typically less than -100 dB $\cdot\text{Hz}^{-1}$ at Fourier frequencies higher than 1 Hz, less than -135 dB $\cdot\text{Hz}^{-1}$ at Fourier

frequencies higher than 100 kHz and less than $-160 \text{ dB}\cdot\text{Hz}^{-1}$ at Fourier frequencies higher than 1 MHz. The frequency noise has been measured against a Fabry-Perot cavity (cavity in vacuum, with INVAR spacer, 10000 finesse). The frequency of the light from the laser is frequency shifted with a 150 MHz acousto-optic modulator (AOM) and sent to the cavity, whose resonance is detected using the Pound-Drever-Hall method [28].

A fast voltage controlled oscillator (VCO) driving the AOM is used to lock to the cavity with a bandwidth greater than 1 MHz. Within the locking bandwidth, the frequency of the RF signal delivered by the VCO reflects frequency fluctuations between the laser and the analyzing cavity. This signal is analyzed with a frequency-to-voltage converter or a RF spectrum analyzer. Fig. 3 shows the laser noise power spectral density (PSD) deduced from these measurements. The linewidth deduced from this measurement, based on the integral of the phase noise PSD, is 3 kHz.

4.2. REFERENCE CAVITY

The clock laser based on a Yb-doped fiber laser at 1062.5 nm is stabilized to an ultra stable Fabry-Perot reference cavity. The design of this system is inspired by previous work reported for instance in [29–32]. This is a vertical cavity placed inside double vacuum chambers and double heat shielding connected to external radiators as is shown in Fig. 4. To minimize thermal noise on the mirrors the fused silica mirrors are used. Design considerations of the cavity for reduced acceleration sensitivity will be given in the other paper. Further details on the mounting scheme will be given also. The Cavity is placed on a passive anti-vibration table inside an anti-acoustic box. Much effort has been devoted to achieve high passive temperature stability to counter balance the higher temperature sensitivity arising from the fused silica (rather than ULE) mirrors. We have measured the finesse of this Fabry-Perot cavity to be $\sim 914\,800$ using the cavity ring down measurement method. Characterization of the fiber laser stabilized to this cavity will be reported elsewhere.

Amplification of this ultra stable source and subsequent frequency quadrupling is reported in the next section.

4.3. 265.6 nm FREQUENCY GENERATION

The first step to generate the 265.6 nm radiation is to amplify the ultra stable light at 1062.5 nm. This is done using a DFB (distributed feedback) semiconductor laser delivering up to 500 mW at this wavelength (250 mW practically usable after the necessary optical isolators, due to a poor mode quality). This laser is stabilized

to the ultra stable light source either by a phase-lock loop (for tunability during preliminary work) or by injection-locking (for clock operation with low noise). The phase noise between the injection-locked DFB laser and the seed fiber laser has been tested (see Fig. 5). Noise in this measurement is limited by the measurement system (electronic noise, uncompensated free space propagation of laser beams, etc). The noise added in the injection-locking process is negligible for our application. The output of the DFB laser diode is frequency doubled twice. First doubling is realized with a 20 mm long PP-KTP crystal. The build-up cavity has a 8% input coupler and a waist in the crystal of $\sim 36 \mu\text{m}$. The measured overall conversion efficiency is 64% which leads to 160 mW at 531 nm.

The second doubling cavity is similar to the one described in Section III. 5 mW of 265.6 nm radiation are generated, conversion efficiency being currently limited by the loss in one of the build-up cavity mirrors. Note, however that this power should be sufficient for the preliminary investigation of the clock transition. Both cavities are currently locked by modulating the cavity length at 31.5 kHz through a PZT driven mirror also used to apply the feedback loop corrections. This method implies that a small phase modulation is imprinted into the clock laser beam. Although this will not be a problem on the short term, high performance clock operation might require the use of a different locking scheme (such as the Hansch-Couillaud scheme [33]) to remove this modulation. Fig. 5 shows the measured RIN of the 265.6 nm light. The observed noise level will not be a limiting factor even for future clock operation at very high stability.

CONCLUSION

We have presented some features of neutral mercury that are making it an interesting candidate for a new optical lattice clock. We have reported on our on going effort to develop such an atomic clock. Sufficient laser power at the laser cooling wavelength of 254 nm has been obtained. Saturated absorption spectroscopy has also been observed and used to stabilize the laser source as required for laser cooling. The vacuum system is now ready for operation after the proposed solutions for controlling the mercury vapour pressure have been successfully tested. Generation of 265.6 nm light for the clock transition by frequency quadrupling a 1062.5 nm source has been implemented with the appropriate power level. The development of an ultra stable reference at 1062.5 nm was realized.

Acknowledgment. The authors would like to acknowledge support from SYRTE technical services. SYRTE is Unité Mixte de Recherche du CNRS (UMR CNRS 8630). SYRTE is associated to Université Pierre et Marie Curie. This work is partly funded by the cold atom network IFRAF. This work received partial support from CNES.

REFERENCES

1. W. H. Oskay, S. A. Diddams, E. A. Donley, T. M. Fortier, T. P. Heavner, L. Hollberg, W. M. Itano, S. R. Jefferts, M. J. Delaney, K. Kim, F. Levi, T. E. Parker, J. C. Bergquist, "Single-atom optical clock with high accuracy," *Physical Review Letters*, **97**, 2, p. 020801, 2006. [Online]. Available: <http://link.aps.org/abstract/PRL/v97/e020801>.
2. M. M. Boyd, A. D. Ludlow, S. Blatt, S. M. Foreman, T. Ido, T. Zelevinsky, J. Ye, "[sup 87] Sr lattice clock with inaccuracy below 10[sup -15]," *Physical Review Letters*, **98**, 8, p. 083002, 2007. [Online]. Available: <http://link.aps.org/abstract/PRL/v98/e083002>.
3. P. Lemonde *et al.*, "An optical lattice clock with spin-polarized 87Sr atoms," in *Proceedings of the 2007 EFTF-FCS conference*, 2007.
4. T. M. Fortier, N. Ashby, J. C. Bergquist, M. J. Delaney, S. A. Diddams, T. P. Heavner, L. Hollberg, W. M. Itano, S. R. Jefferts, K. Kim, F. Levi, L. Lorini, W. H. Oskay, T. E. Parker, J. Shirley, J. E. Stalnaker, "Precision atomic spectroscopy for improved limits on variation of the fine structure constant and local position invariance," *Physical Review Letters*, **98**, 7, p. 070801, 2007. [Online]. Available: <http://link.aps.org/abstract/PRL/v98/e070801>.
5. H. Katori, M. Takamoto, V. Pal'chikov, V. Ovsiannikov, "Ultrastable optical clock with neutral atoms in an engineered light shift trap," *ArXiv:physics/0309043*, 2003.
6. M. Takamoto, H. Katori, "Spectroscopy of the s[sub 0] - p[sub 0] clock transition of sr in an optical lattice," *Physical Review Letters*, **91**, 22, p. 223001, 2003. [Online]. Available: <http://link.aps.org/abstract/PRL/v91/e223001>
7. E. J. Angstromann, V. A. Dzuba, V. V. Flambaum, "Relativistic effects in two valence-electron atoms and ions and the search for variation of the fine-structure constant," *Physical Review A (Atomic, Molecular, and Optical Physics)*, **70**, 1, p. 014102, 2004. [Online]. Available: <http://link.aps.org/abstract/PRA/v70/e014102>
8. Chapelet *et al.*, "Comparisons between 3 fountain clocks at LNESYRTE," in *Proceedings of the 2007 EFTF-FCS conference*, 2007.
9. S. Bize, P. Laurent, M. Abgrall, H. Marion, I. Maksimovic, L. Cacciapuoti, J. Gr'unert, C. Vian, F. Pereira dos Santos, P. Rosenbusch, P. Lemonde, G. Santarelli, P. Wolf, A. Clairon, A. Luiten, M. Tobar, C. Salomon, "Advances in ¹³³Cs fountains," *C. R. Physique*, Vol. 5, p. 829, 2004.
10. F. E. Poindexter, "Mercury vapor pressure at low temperatures," *Physical Review*, **26**, 6, pp. 859-868, 1925. [Online]. Available: <http://link.aip.org/link/?PR/26/859/1>.
11. M. Bignon, "Probabilite de transition de la raie 6 1S0-6 3P0 du mercure," *Journal de Physique*, **28**, p. 51, 1967.
12. V. Pal'chikov, Private Communication, 2004.
13. V. D. Ovsiannikov, V. G. Pal'chikov, H. Katori, M. Takamoto, "Polarisation and dispersion of light shifts in highly stable optical frequency standards," *Quantum Electronics*, **36**, p. 3, 2006.
14. Z. W. Barber *et al.*, *Phys. Rev. Lett.*, **96**, 083002 (2006).
15. S. G. Porsev, A. Derevianko, *Phys. Rev.*, **A 74**, 020502 (2006).
16. E. J. Angstromann *et al.*, *Phys. Rev.*, **A 70**, 014102 (2004).
17. *. <http://physics.nist.gov/PhysRefData/Handbook/Tables/mercurytable1.htm>.
18. P. *et al.*, "Black body radiation shift in primary frequency standards," in *Proceedings of the 2007 EFTF-FCS conference*, 2007.
19. S. G. Porsev, A. Derevianko, "Multipolar theory of blackbody radiation shift of atomic energy levels and its implications for optical lattice clocks," *Physical Review A (Atomic, Molecular, and Optical Physics)*, **74**, 2, p. 020502, 2006. [Online]. Available: <http://link.aps.org/abstract/PRA/v74/e020502>.
20. T. Rosenband, W. M. Itano, P. O. Schmidt, D. B. Hume, J. C. J. Koelemeij, J. C. Bergquist, D. J. Wineland, "Blackbody radiation shift of the 27a1+ 1s0-3p0 transition," *arXiv:physics/0611125v2*, 2006.

21. V. Pal'chikov *et al.*, "Optical lattice polarization effects on hyperpolarizability of alkaline-earth atoms," in *Proceedings of the 2007 EFTF-FCS conference*, 2007.
22. K. Dieckmann, R. J. C. Spreeuw, M. Weidemüller, J. T. M. Walraven, "Two-dimensional magneto-optical trap as a source of slow atoms," *Phys. Rev.*, **A 58**, 5, pp. 3891–3895, Nov. 1998.
23. D. Berkeland, F. Cruz, J. Bergquist, "Sum-frequency generation of continuous-wave light at 194 nm," *Applied Optics*, **36**, p. 4159, 1997.
24. M. Scheid, F. Markert, J. Walz, J. Wang, M. Kirchner, T. W. Hansch, "750 mw continuous-wave solid-state deep ultraviolet laser source at the 253.7 nm transition in mercury," *Optics Letters*, **32**, 8, pp. 955–957, Apr. 2007.
25. I. Courtillot, A. Quessada, R. Kovacich, A. Brusch, D. Kolker, J.-J. Zondy, G. Rovera, P. Lemonde, "Clock transition for a future optical frequency standard with trapped atoms," *Phys. Rev. A* **68**, p. 030501, 2003.
26. C. W. Hoyt, Z. W. Barber, C. W. Oates, T. M. Fortier, S. A. Diddams, and L. Hollberg, "Observation and absolute frequency measurements of the $[^1\text{s}^0]-[^3\text{p}^0]$ optical clock transition in neutral ytterbium," *Physical Review Letters*, **95**, 8, p. 083003, 2005. [Online]. Available: <http://link.aps.org/abstract/PRL/v95/e083003>.
27. * * The Yb-doped fiber laser is from Koheras.
28. R. Drever, J. Hall, F. Kowalski, J. Hough, G. Ford, A. Munley, H. Ward, "Laser phase and frequency stabilization using an optical resonator," *Appl. Phys.*, **B 31**, p. 97, 1983.
29. B. Young, F. Cruz, W. Itano, J. Bergquist, "Visible lasers with subhertz linewidths," *Phys. Rev. Lett.*, **82**, p. 3799, 1999.
30. S. A. Webster, M. Oxborrow, P. Gill, "Vibration insensitive optical cavity," *Physical Review A (Atomic, Molecular, and Optical Physics)*, **75**, 1, p. 011801, 2007. [Online]. Available: <http://link.aps.org/abstract/PRA/v75/e011801>.
31. C. T. Taylor, M. Notcutt, D. G. Blair, "Cryogenic, all sapphire, fabry-perot optical frequency reference," *Review of Scientific Instruments*, **66**, 2, pp. 955–960, 1995. [Online]. Available: <http://link.aip.org/link/?RSI/66/955/1>.
32. L. Chen, J. L. Hall, J. Ye, T. Yang, E. Zang, T. Li, "Vibration-induced elastic deformation of fabry-perot cavities," *Physical Review A (Atomic, Molecular, and Optical Physics)*, **74**, 5, p. 053801, 2006. [Online]. Available: <http://link.aps.org/abstract/PRA/v74/e053801>.
33. T. Hansch, B. Couillaud, "Laser frequency stabilization by polarization spectroscopy of a reflecting reference cavity," *Opt. Commun.*, **35**, p. 441, 1980.